ORIGINAL PAPER

Biomechanical analysis of the upper body during overhead industrial tasks using electromyography and motion capture integrated with digital human models

Dario Panariello[1,2] · Stanislao Grazioso[1] · Teodorico Caporaso[1] · Angela Palomba[3] · Giuseppe Di Gironimo[1] · Antonio Lanzotti[1]

Abstract

In this paper, we present a biomechanical analysis of the upper body, which includes upper-limb, neck and trunk, during the execution of overhead industrial tasks. The analysis is based on multiple performance metrics obtained from a biomechanical analysis of the worker during the execution of a specific task, i.e. an overhead drilling task, performed at different working heights. The analysis enables a full description of human movement and internal load state during the execution of the task, thought the evaluation of joint angles, joint torques and muscle activations. A digital human model is used to simulate and replicate the worker's task in a virtual environment. The experiments were conduced in laboratory setting, where four subjects, with different anthropometric characteristics, have performed 48 drilling tasks in two different working heights defined as low configuration and middle configuration. The results of analysis have impact on providing the best configuration of the worker within the industrial workplace and/or providing guidelines for developing assistance devices which can reduce the physical overloading acting on the worker's body.

Keywords Industry · Overhead tasks · Ergonomics · Biomechanics · Electromyography · Digital human models

1 Introduction

Overhead tasks are very common in assembly lines of automotive and aerospace industries and in daily tasks for construction workers. In industrial settings, they are complex and usually involve the production of multiple variants of the same product; being difficult to automate, overhead tasks are mostly performed by workers. In these scenarios, the manipulation abilities and cognitive skills of the worker are essential to successfully complete the task.

The execution of overhead tasks involves different parts of the upper body (i.e. upper-limb, neck and trunk); this increases the risk associated to work-related musculoskeletal disorders (WMSD). It is important to underline that, according to Schneider et al. in [1], among all WMSD, almost 45% afflicts the upper-limbs and 38% the trunk and back. In this work, we focus on drilling overhead tasks, as they have been defined as the most demanding industrial overhead tasks for the workers [2].

Over the last decade, the most adopted approaches for evaluating the risks associated to WMSD have been: Ovako Working Posture Analysing System (OWAS) [3], Rapid

✉ Giuseppe Di Gironimo
  giuseppe.digironimo@unina.it

  Dario Panariello
  dario.panariello@unibg.it

  Stanislao Grazioso
  stanislao.grazioso@unina.it

  Teodorico Caporaso
  teodorico.caporaso@unina.it

  Angela Palomba
  angela.palomba@unicampania.it

  Antonio Lanzotti
  antonio.lanzotti@unina.it

1   Department of Industrial Engineering, University of Naples Federico II, 80125 Naples, Italy

2   Department of Management, Information and Production Engineering, University of Bergamo, 24044 Dalmine, Italy

3   Department of Medical and Surgical Specialties and Dentistry, University of Campania Luigi Vanvitelli, 80138 Naples, Italy

Upper Limb Assessment (RULA) [4] and Rapid Entire Body Assessment (REBA) [5]. These methods consider the working posture of the worker during the execution of the task, then assign a score for each part of the body and a final score which expresses the ergonomic condition of the worker. In particular, OWAS and REBA consider the human joints of the whole body; instead, RULA considers only the human joints of upper body. However, these approaches present some limitations: (i) the methods can only be used for static works; (ii) they allow to make an overall ergonomic evaluation of the task, but they do not allow to identify the parts of the body (joints and muscles) which are mostly stressed by the task; (iii) they provide a rough final score, in the sense that only large angular variations of the human joints can cause a variation of final score. In summary, the empirical methods do not allow to have a complete analysis of the industrial task; this can be a problem mainly for complex tasks as the overhead tasks [6]. To overcome these limits, a posture evaluation together with a biomechanical analysis is required: this allows a deeper understanding of workers motion and ergonomics during the execution of industrial tasks [7]. In the literature, there is a limited evidence of biomechanical analysis of whole upper body during the execution of overhead drilling tasks. The available studies are indeed focused on the effects of working height only on shoulder torque and muscle activities of the upper-limb [8,9]. However, overhead drilling tasks, apart from upper-limb, also involves different part of the upper body, i.e. trunk.

Recent methods have been proposed by the authors to design user-centered wearable systems [10] and adaptable workplaces [11]. The idea of methods presented is to include the ergonomic and biomechanical assessments since the beginning of the design process of custom wearable devices and industrial workplaces. In this paper, the method presented in [11] is used to perform the biomechanical analysis of the whole upper body during the execution of the most demanding overhead task, i.e. drilling. In particular. multiple performance metrics are derived to have a complete view of the worker biomechanical behavior of upper body, i.e. upper-limb, neck and trunk, during the execution of the task, with the objective to understand the real sources of WMSD. In particular, the performance metrics include: average timing values of the task execution, temporal profiles and average of joint angles, average of joint torques, root mean square of the normalized muscle activations. The evolution over time of the joint angles and joint torques are evaluated reproducing the movement of the worker in virtual scenario using digital human models (DHM), i.e. OpenSim [12]; the muscle activations, instead, are computed from the electromyographic (EMG) signals. The analysis is also compared with the most used approach for evaluation of overhead works, i.e. RULA checklist, and with compering works. The results confirm that only an integrated approach can be effectively used to

define the biomechanical behaviour of the worker, and thus provide guidelines for ergonomic design of industrial workstations and, rational selection or development of assistance aids (i.e. robotic exoskeletons), if needed for the task.

The paper is organized as follows. Section 2 illustrates the performance metrics and the tools used for biomechanical analysis. Section 3 describes the experiments, while Sect. 4 illustrates the results. Section 5 provides a long discussion, including the comparison with the RULA method and past works, possible exploitation of the results of this study and its limitations. Finally, the conclusions are given in Sect. 5.

2 Methods

In the biomechanical analysis of the upper body we consider four aspects: (1) task performance; (2) kinematic movements; (3) dynamic loads; (4) muscle activities. For each aspect, a performance measure is derived. The biomechanical analysis is based on the reconstruction of joint angles and torques from motion capture and ground reaction forces data using biomechanical modeling, and estimation of muscle activation from surface electromyography. The overall methodology used in this work is illustrated in Fig. 1.

2.1 Multiple performance metrics

2.1.1 Task performance

Classic metrics used to evaluate the task performance are: (i) number of repetitions during a time period [13]; (ii) time to reach a specific target which represents the work position [2]; (iii) execution time of the task [9,14–16]. In real factory scenarios, workers are usually instructed to perform a task in the shortest possible time, to enhance productivity. Therefore, our task performance metric is the execution time of the task.

2.1.2 Kinematic movements

With movements we refer to kinematics and posture of the worker during the execution of an industrial task. Common metrics used to measure workers movement are: (i) range of motion (RoM) of workers during the execution of a task [15,16]; (ii) maximal or average value [2]; (ii) temporal profiles, i.e. evolution over time of the joint angles of the workers [2]. In this work, we use an average values of joint angles since the task can be considered static task. Moreover, we use a pairwise comparison of joint angles, as proposed in [17], to evaluate the the influence of each joint on the specific industrial task. Finally, we report the temporal profiles of joint angles to validate the results obtained for the selected task and to take into account the variation of the joints not visible
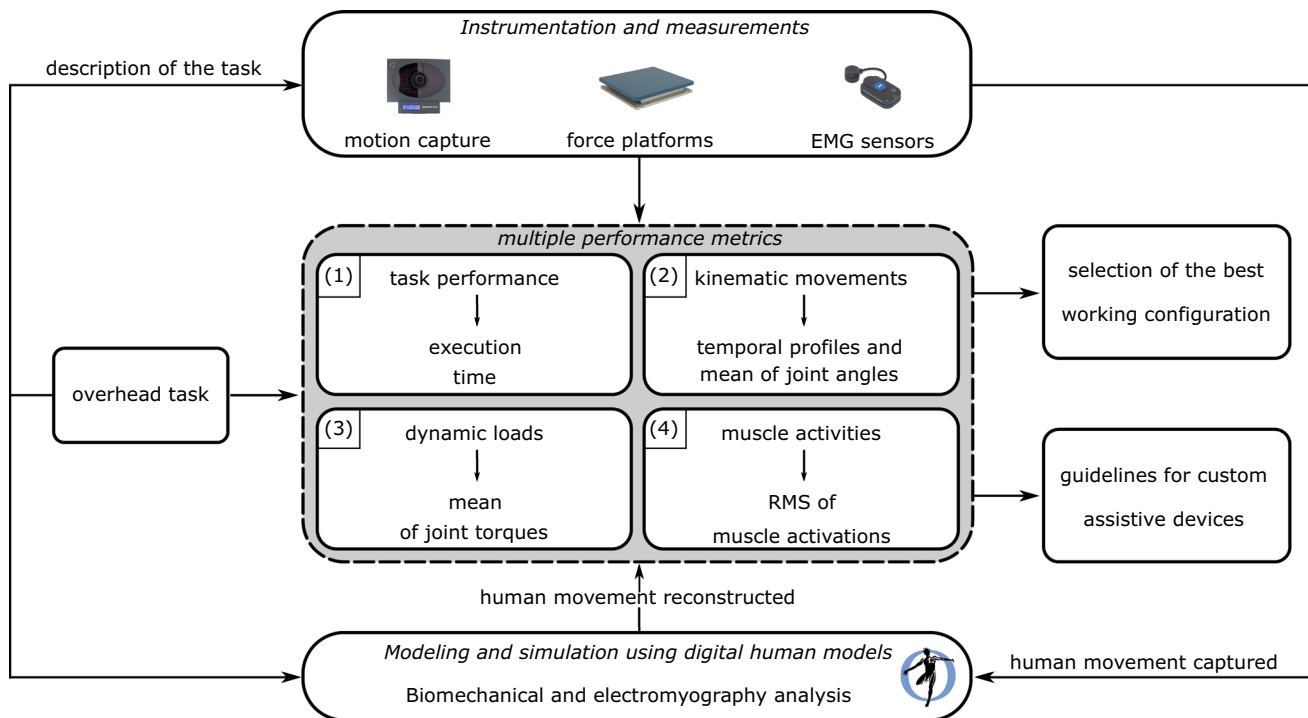
Fig. 1 Biomechanical analysis of the industrial task to reduce the risks associated to WMSD

through the selected metrics. The joint angles are reconstructed using inverse kinematics (see, e.g. "Appendix A.1").

2.1.3 Dynamic loads

The loading of each joints during the execution of an industrial task can be evaluated in static and dynamic conditions: (i) static joint loads using average values [15] and static joint torques using temporal profile [18,19]; (ii) dynamic torques using average values [16]. Since industrial tasks often involve the use of tools which generate vibrations (e.g. drilling tasks), in this work we use the average values of joint torques as dynamic performance metric. Dynamic analysis are therefore useful to establish the configuration of the workstation which minimize the joint torques on the workers. The joint torques are reconstructed using inverse dynamics (see, e.g. "Appendix A.2").

2.1.4 Muscle activities

The muscle activities are usually quantified with a direct measure of muscle activations [2,9,20,21]. The EMG signals can be studied in: (i) time domain, using the average or root mean square (RMS) values of the signal [20,21]; (ii) frequency domain, using mean power frequency (MPF) or median power frequency (MDF) [9]. In this work, we use the time domain to have a perfect correlation between muscle activation and kinematic/dynamic results. In particular,

we select root mean square (RMS) values of muscle activations to characterize the muscle activities of the worker and to define the part of the body subject to the largest physiological demand during the activity. The calculation of this metric requires specific protocol (see Sect. 3.5.2) for treatment and processing of EMG signals.

2.2 Biomechanical analysis of workers

2.2.1 Human movements capturing

Classic technologies used for human movements capturing include: (i) optical cameras with markers and without markers [15,22,23]; (ii) wearable motion sensing suits with e.g. inertial measurements units (IMU) [24] and/or soft sensors [25]. For dynamic analysis, instead, the most adopted technologies are: (i) force platforms; (ii) wearable force sensors, e.g. wearable force plates [26]. In industrial settings, wearable motion capture systems and wearable force sensors would be preferable, as the inertial suit Xsens MVN [27] and wearable force sensors as Xsens shoes [28]. However, they present a low accuracy [29] in evaluating human joint angles and torques if compared to laboratory equipment (optical cameras and force platforms), which currently are the most accurate systems for tracking human motions. In this work, we use optical cameras with markers and force platforms in order to obtain results as accurate as possible. Finally, muscle

activations are measured using surface EMG (sEMG) sensors as proposed in the literature [2,9,20,21].

2.2.2 Human movements reconstruction

Digital human models (DHM) are used to describe the behaviour of the subject from the human motion data, and they are used to replicate the human activity in virtual environment. Classic software used in this context can be divided in: (i) static DHM software (as Simens Tecnomatix Jack [30], an application for industrial tasks are illustrated in [31]); (ii) biomechanical-based DHM software which implements biomechanical models of the human body with an accurate dynamic analysis (as AnyBody [32] and OpenSim [12]). For a comprehensive overview of DHM and associated software tools, the reader can refer to [33]. One of the most used biomechanical-based DHM environments is OpenSim, an open source software. Here, simulations are generated by experimentally measured kinematic, kinetic and EMG patterns. This software, initially devoted mainly to medical and sports applications, has recently demonstrated interesting capabilities in risk-assessment of WMSD [6,34]. Therefore, we use OpenSim also in this work. The basic advantages of OpenSim are: (i) scaling of the digital human model (DHM) based on real anthropometric characteristics; (ii) generating a muscle-driven simulation of human movements; (iii) computing of DHM joint angles, torques and muscle activations. The detailed procedures for inverse kinematics and inverse dynamics starting from motion capture and ground reaction forces data are reported in "Appendix A". However, in this study we compute the muscle activation directly by the EMG signals, in order to obtain a more manageable and accurate analysis of the human muscle activities.

3 Experiments

A laboratory study on a drilling overhead task performed at different working heights was conducted according to literature indications [9,13,14] and the technical characteristics of the case study, see e.g. Sect. 3.2. The objective of the experiments is to evaluate the multiple performance metrics, reported in Sect. 2, of the upper body during the execution of a specific overhead task. The experiments were performed at ErgoS Lab, the Laboratory of Advanced Measures on Ergonomics and Shapes at CeSMA, University of Naples Federico II.

3.1 Participants

Four right-hand Italian males, volunteer subjects, were selected from the local population to participate for the experiments. The subjects do not have or have limited experience

with industrial work. All participants did not report any musculoskeletal disorders or problems over the past twelve months. Participants gave written informed consent, according to the Statement of Ethics Committee of University of Naples Federico II—Ref. Protocol 335/20, before starting the experiments. After an initial briefing, a physician collected their anthropometric characteristics and personal details: these are reported in Table 1. According to the Italian population stature distribution [35], two subjects belong to the 97th percentile (in the following referred to with the letters a and b), while two subjects belong to the 50th percentile (in the following referred to with the letters c and d) as proposed in [36].

3.2 Case study

The case study is a drilling overhead task, very common in industry. An example of the task as performed in a automotive work environment is illustrated in Fig. 2. The worker typically performs the tasks standing with the right hand above the head while the car is on the lift bridge. The lift bridge allows the vertical translation, in order to realize an adjustable working height based on the anthropometric characteristic of the worker. The technical details of a generic overhead task for a full shift reported in [37]. In particular, this study indicates that the duration of the shift is equal to 9 hours, with 4 brake times of 15 minutes and 1 brake time of 30 minutes; the length of a single trial, which includes n repetitions of the same operation, is about 100 seconds. The overhead drilling task, as illustrated above, was reproduced in laboratory settings (see Sect. 3.3) in order to obtain accurate and reliable measurements for the selected performance metrics.

3.3 Laboratory task setup and description

Task setup An experimental platform for performing overhead tasks with different working heights was designed (see, e.g. Fig. 3) simulating the working environment shown in Fig. 2: it is composed of four circular section poles (height-adjustable), which support an overhead platform composed by a rectangular structure (square section).

Task description The subjects were asked to stay with the right hand below the head for about 7 seconds (reset position) and to drill a wooden beam (dimension: 70x70 mm) with a drill having a wood tip of diameter 10 mm (working posture). The weight of the drill is 1850 g. Each trial consisted in three repetitions of the operations (work cycles) with an average duration of 14 seconds and a pause between two work cycles of 7 seconds in order to obtain a duration of about 56 seconds. Moreover, the time spent by the subject to position himself correctly below the platform for the drilling task, raising and lowering the arm, as well as picking up the

Table 1 Anthropometric characteristics: height, weight, Uarm (upper arm), Larm (lower arm) and personal detail (i.e., age) of the subjects involved for the experiments

	Age (yr)	Height (cm)	Weight (kg)	Uarm (cm)	Larm (cm)
Mean	27.0	182.1	84.9	36.6	26.9
S.D.	5.0	6.8	8.5	0.8	2.7
Min.	24.0	176.0	77.0	36	23.5
Max.	34.0	189.0	95.4	37.5	29.0

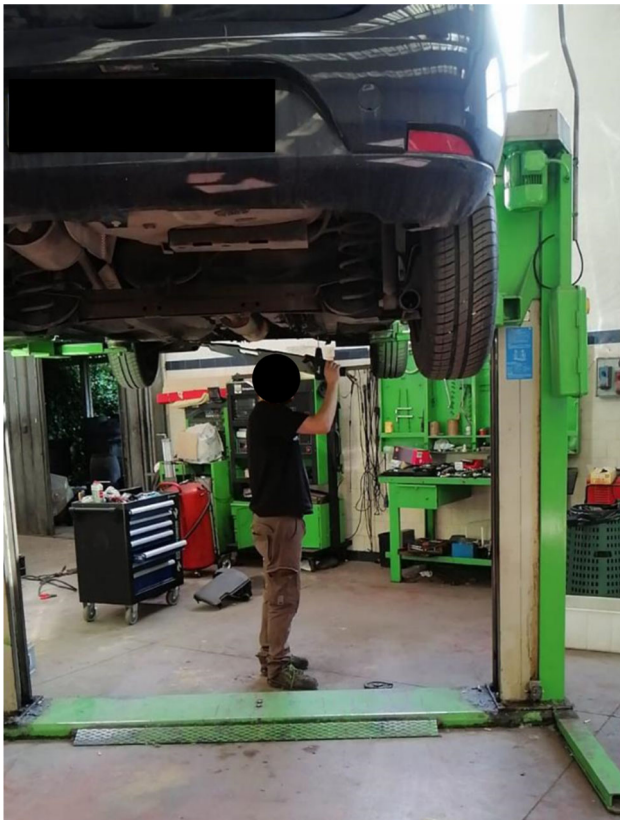*S.D.* standard deviation, *Min.* minimum value, *Max.* maximum value

Fig. 2 Demonstration of overhead drilling task in a work environment

Fig. 3 Front view of the experimental setup comprising four poles as based and overhead platform to perform drilling task
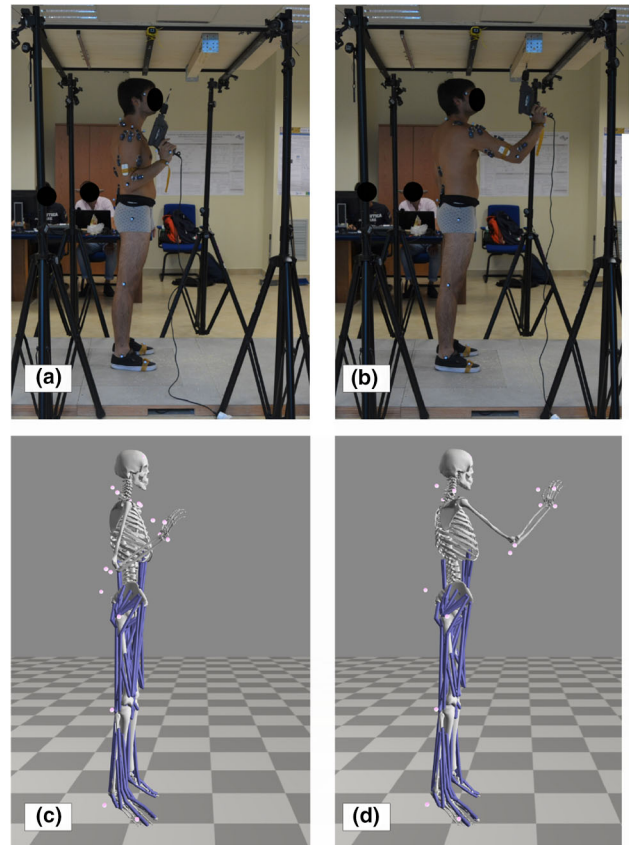

Fig. 4 Basic postures in performing the drilling task: **a**, **b**: real pictures; **c**, **d**: OpenSim model. **a** and **c** reset posture; **b** and **d** working posture
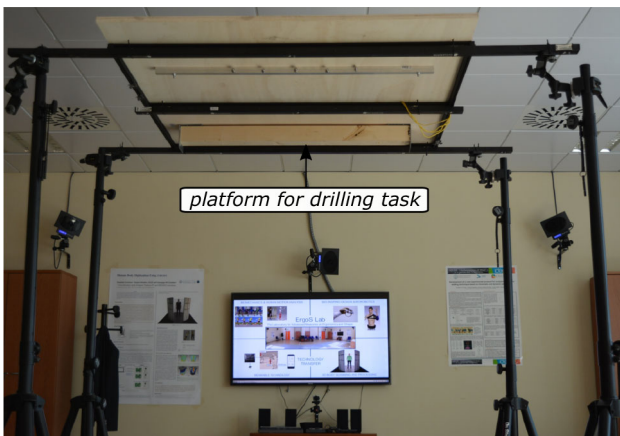
tool, takes about 60 seconds for a total of about 106 seconds per trial as indicated in [37]. The reset and working positions of the drilling overhead task are shown in Fig. 4.

Independent variable The independent variable of the experiment was the height of the platform for drilling task. In particular, the task was replicated at two different working heights, called in the following *low configuration* and *middle configuration*. The working height h depends on the anthropometric characteristics of the subjects, and is defined as:

$$h = A + n(B - A) \qquad (1)$$

where A: lowest possible working height for the selected task (see Fig. 5) and defined in [9] as: "hand height with the
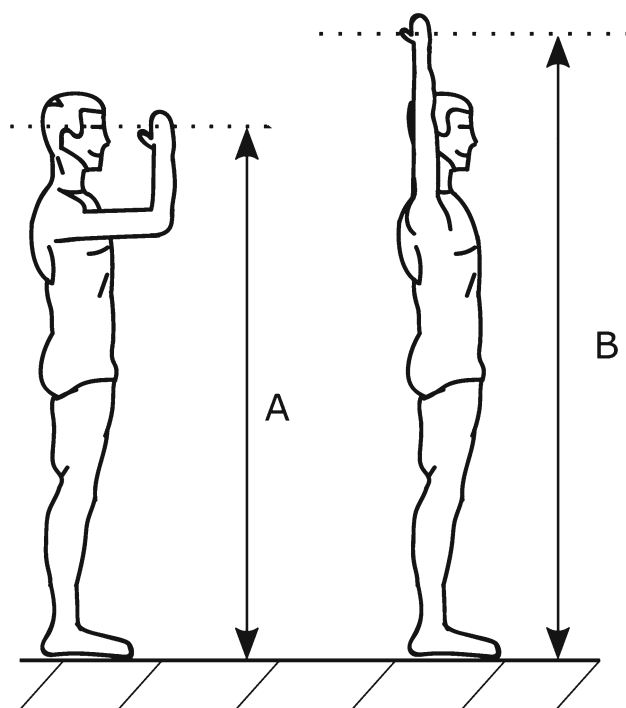
Fig. 5 Side view of the two anthropometric characteristics selected to evaluate the working height configurations defined in [9]

shoulder and elbow fixed to 90 degrees in neutral upper arm rotation"; B: highest possible working height for the selected task (see Fig. 5) and defined in [9] as "hand height with the upper arm in full flexion (maximum overhead reach) with shoulders parallel to ground"; n: weight coefficient, it can assume values between 0 and 1.

In our experiments, we have used two working heights: h_1, using $n = 0$ (low configuration) and h_2, using $n = 0.4$ (middle configuration), as proposed in [9]. For each working height, we have performed two trials; the recovery time between two consecutive tests was chosen equal to 50% of the duration of the test. Since four subjects were involved for two trials of three work cycles each, a total of 48 experiments have been performed.

3.4 Instrumentation

This section describes the sensors and equipment used to measure human parameters related to the biomechanical measures described in Sect. 2.

Motion capture system The system used in the experiments to track the kinematics is a motion capture system composed by ten infrared digital cameras (SMART DX 6000, BTS Bioengineering). The sampling frequency of the cameras is 340 Hz, at their maximum resolution of 2048×1088 pixel.

Ground reaction forces Eight integrated force platforms (P-600, BTS Bioengineering) with sample frequency of 680 Hz are used for ground reaction forces measurements.

Surface electromyography Muscle activities are measured by using eight EMG sensors (FREEEMG 1000 and 300, BTS Bioengineering).

3.5 Protocols

Two different protocols were defined to track human joint angles and to measure the human muscle activations. One physician was involved in this study to guarantee the correct placement of the markers and EMG sensors on the human body.

3.5.1 Marker protocol

For the overhead task, we used an ad-hoc measurement protocol composed of twenty-two markers. The protocol includes twelve markers placed on the upper body according to the work in [38] and, additionally, two markers on the hand according to [39]. The latter two markers have been added in the marker protocol as they allow to define and calculate the wrist angles during the execution of the industrial task. With respect to [38], the two additional markers on the anterior superior iliac spine and four markers placed on the left arm were excluded since the subjects involved in the current experiments are all right-handed, and thus these markers are not needed. The last eight markers were placed on the lower body of the subject according to palpable anatomical landmarks on the lower extremity used in [40]. The full marker set is illustrated in Fig. 6.

The defined marker protocol allows to reconstruct the following joint angles and the relative joint torques:

- Upper-limb angles/torques which includes shoulder flexion–extension (α/τ_1) and abduction–adduction (β/τ_2);
- Lower limb angles/torques which includes shoulder rotation (γ/τ_3) and elbow flexion–extension (δ/τ_4);
- Wrist angles/torques which includes wrist flexion–extension (ϵ/τ_5), wrist radial–ulnar deviation (ζ/τ_6) and pronation–supination (η/τ_7);
- Trunk angles/torques which includes trunk flexion–extension (θ/τ_8), lateral bending (ι/τ_9) and axial rotation (κ/τ_{10});
- Neck angles/torques which includes neck flexion–extension (λ/τ_{11}), axial rotation (μ/τ_{12}) and lateral bending (ν/τ_{13}).

3.5.2 EMG protocol

The EMG sensors were placed on the upper body of the subjects according to [20,41] and following to the indications
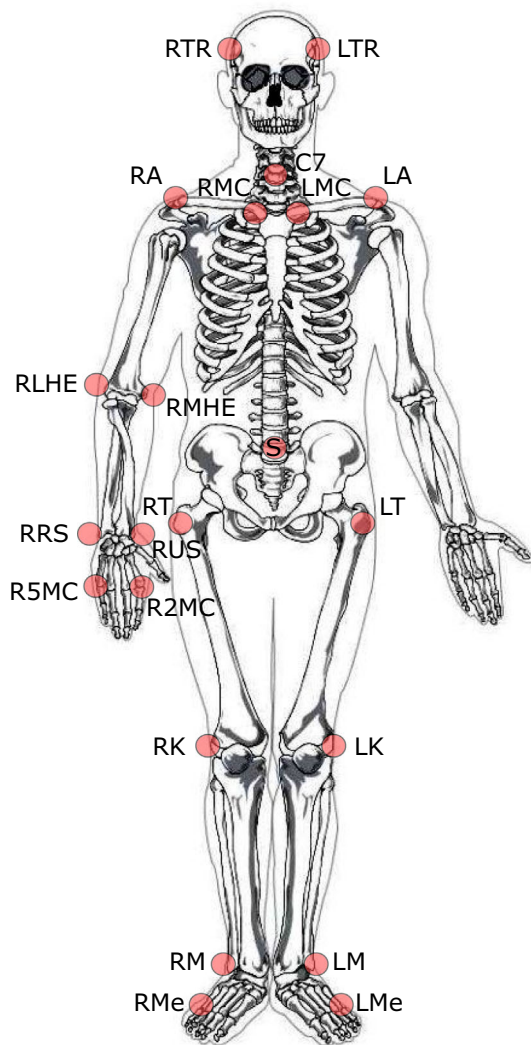
Fig. 6 Marker set on the human body, where: *LTR/RTR* left/right temporal regions, *LMC/RMC* left/right medial end of the Clavicle, *C7* cervical vertebra, *LA/RA* left/right acromion, *RLHE/RMHE* right lateral/medial humeral epicondyle, *RRS/RUS* right radial/ulnar styloid, *R2MC/R5MC* right 2nd/5th metacarpal, *S* sacrum, *LT/RT* left/right greater trochanter, *LK/RK* left/right lateral femoral epicondyle, *LM/RM* left/right malleolus, *LMe/RMe* 5th metatarsal of the left/right foot

Table 2 Positions of EMG sensors on the human muscles

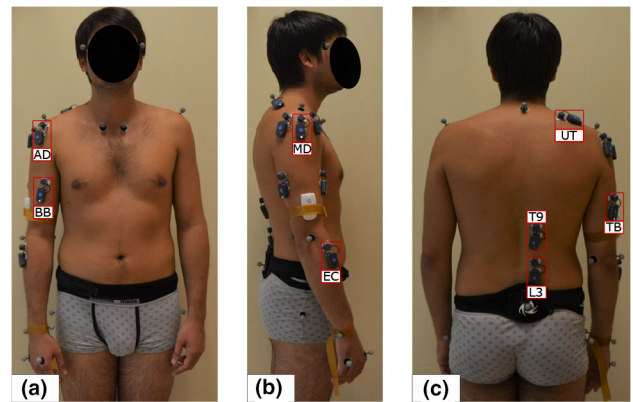| Body muscles	EMG sensor position
Shoulder or neck	Anterior deltoid (AD)
Shoulder or neck	Medial deltoid (MD)
Shoulder or neck	Upper trapezium (UT)
Arm or hand	Biceps Brachii (BB)
Arm or hand	Long head of the triceps Brachii (TB)
Arm or hand	Extensor Carpi radials longus (EC)
Trunk or lower back	Erector spinae at level L3 ($L3$)
Trunk or lower back	Erector spinae at level T9 ($T9$)

Fig. 7 Marker and EMG sensors on the subject's body. **a–c** Front view; **b** side view

given by the SENIAM project.[1] The muscles included in the study are summarized in Table 2; the positions of the EMG sensors on real subject are shown in Fig. 7. In particular, the EMG sensors were positioned on the dominant side of the subject (right side for all subjects, see Sect. 3.1).

Before starting the experiments, the participants were asked to perform isometric maximal voluntary contractions (MVC) used to normalize the EMG signals (see Sect. 3.6). The manual muscle tests carried out for each muscle considered, according to SENIAM project, are:

- anterior deltoid (AD): the physician is positioned behind the subject and asks the subject to perform against resistance shoulder abduction in slight flexion, with the humerus in slight rotation;
- medial deltoid (MD): the physician is placed laterally to the subject and resists abduction of the arm to 90 degrees (without rotation);
- upper trapezium (UT): the physician stands behind the subject and unilateral action resists shoulder elevation and tilt of the head;
- biceps brachii (BB): the physician stands in front of the subject and resists elbow flexion (with the forearm in supination);
- long head of the triceps brachii (TB): the physician stands in front of the subject and resists elbow extension;
- extensor carpi radials longus (EC): the physician stands in front of the subject and resists the wrist extension (with his hand closed in a fist);
- erector spinae at level L3 and T9 ($L3$ and $T9$): the subject was asked to lift the trunk against resistance from a prone position.

---

[1] http://www.seniam.org.

3.6 Data processing and analysis

The marker positions, the ground reaction forces and muscle activations during the task execution were captured and processed using BTS SMART Capture and BTS SMART Analyzer software (BTS Bioengineering, Milan, Italy). Kinematics and dynamics were reconstructed using OpenSim. Then, the results of inverse kinematics, inverse dynamics as well as muscle activations were imported in MATLAB (MathWorks, Natick, USA) to identify the temporal events of the tasks and to perform the statistical analysis of the results. *Kinematics and dynamics* The evolution over time of the joint angles and torques specified in Sect. 3.5.1 were reconstructed using biomechanical musculoskeletal models available in OpenSim [12]. According our knowledge, a full model which considers all the joint angels and torques of our interest is not available in OpenSim. Therefore, we have used two different models: (i) *Full-Body Musculoskeletal Model* [42]; (ii) *Musculoskeletal Model of Head* [43]. The first model, usually used for full-body analysis, includes 37 degrees-of-freedom (DoF); among these, 7 DoF are available for each upper-limb. Through this model we were able to reconstruct the evolution over time of the angles and torques of: upper limbs, lower limbs and trunk. The second model, indeed, was used to reconstruct the angles and torques of the neck. Each OpenSim model, at the beginning, was scaled in accordance with the anthropometric characteristics of the subjects (as specified in Sect. 3.1). Figure 4 shows the virtual simulation of the human model during the virtual execution of the drilling task in OpenSim. The details about the inverse kinematics and inverse dynamics computations are available in "Appendix A".

Muscle activations The EMG signals were processed according to the following four steps [44]: (i) rectification; (ii) smoothing with a moving average filter (with time constant of 150 ms); (iii) filtering using a Butterworth low-pass filter with a cut off frequency of 2 Hz; (iv) normalization with respect to the maximum voluntary contractions.

Dependent variables The dependent variables evaluated in these experiments are the multiple performance metrics explained and illustrated in Sect. 2.1: i.e. task performance, temporal profile and mean of joint angles of the kinematic movements, mean of the joint torques and root mean square of muscle activations. The dependent variables were evaluated in the two different working heights specified in Sect. 3.3.

Statistical analysis The multiple performance metrics (see Sect. 2.1) are presented as mean ± standard deviation, and the processing was performed using MATLAB. Initially, the data of *low configuration* and *middle configuration* are checked for normality with the Shapiro–Wilk test and then with the Levene's test for homogeneity of variances. The effect of the two working height configurations on mean of joint angles and torques as well as on root mean square of muscle acti-
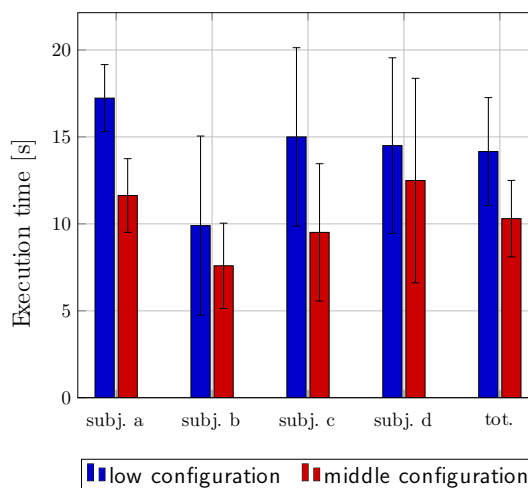

Fig. 8 Average values of execution time for the four subjects (subj. a; subj. b; subj. c and subj. d) in the two working height configurations: *low configuration* and *middle configuration*

vations, were tested with analysis of variance (ANOVA). The level of significance was set equal to 0.05. Finally, the effect size (ES) was calculated only for statistically significant results since the differences between the two working height configurations that depend on the sample fluctuation are not relevant. The ES values for each joint angle, torque and muscle activation at the low and middle working height configurations were calculated according to Cohen's d [45]. In accordance with [45,46], we use the following scale for interpretation of the effect size results: small, for $ES \leq 0.2$; medium, for $0.2 < ES \leq 0.5$; large, for $0.5 < ES \leq 0.8$; very large, $0.8 < ES \leq 1.20$; huge, for $ES > 1.20$.

4 Results

In this section we present the results of the biomechanical analysis of the overhead drilling task, with regards to the metrics defined in Sect. 2.1.

4.1 Task performance

The metric regarding task performance is the execution time of the task, which represents an estimate of productivity. The mean values of the execution time for the four subjects are reported in Fig. 8. Passing from *low configuration* to *middle configuration*, the figure shows a significant decrease, with a large effect, of the execution time of 3.86 s ($p = 0.006$; $ES = 0.800$) which corresponds to a relative decrease of 27.3% and thus, a potential increase of productivity.

4.2 Kinematic movements

We have selected two metrics regarding kinematic movements: temporal profiles of joint angles and average values of joint angles.

Temporal profile The inverse kinematic results in terms of mean $\pm$ standard deviation, i.e. reconstruction of temporal profiles of human joint angles for the two configurations, are plotted in Fig 9. The plots in Fig 9 are in agreement with the selected task; for example, we can see from the first subplot (regarding joint angle α, i.e. shoulder flexion-extension) that the angle α increases passing from the *low configuration* to the *middle configuration*, as expected. We can also see that, during the execution of the task, for each work cycle, the same angle increases since the drilling of the drill bit inside the wooden beam increases. Notice that in these plots we do not include the neck angles (neck flexion-extension, axial rotation and lateral bending) since their variations for the drilling task are not relevant (indeed, these angle variations are around 1 degree). These plots also include the limit values of RULA local score, as these will be useful in Sect. 5.2 for a comparison of the presented strategy with classic ergonomic assessment methods currently used in industry.

Average values of joint angles The evolution over time of the joint angles reported in Fig. 9 shows a constant trend of the pronation–supination and wrist angles. For this reason, we have compared only the joint angles of the upper arm (shoulder flexion–extension and abduction–adduction) and the joint angles of the lower arm (shoulder rotation and elbow flexion–extension), reported in Fig. 10, and trunk angles (trunk flexion–extension, axial rotation and lateral bending), reported in Fig. 11. In particular, we have represented the number of combinations, without repetitions, of k objects from n as following: $C_{n,k} = \frac{n!}{k!(n-k)!}$. For upper arm and lower arm angles the number of combinations are equal to 6 ($C_{4,2} = 6$, see Fig. 10) and for trunk angles the number of combinations are equal to 3 ($C_{3,1} = 3$, see Fig. 11). Observing Figs. 10 and 11, passing from *low configuration* to *middle configuration* we can notice the following results:

– a significant increase, with a huge effect, of the shoulder flexion–extension α of 22.42 degrees ($p < 0.001$; $ES = 2.922$);
– a significant decrease, with a medium effect, of the shoulder abduction–adduction β of 0.62 degrees ($p = 0.0015$; $ES = 0.223$);
– a significant decrease, with a large effect, of the shoulder rotation γ of 2.84 degrees ($p = 0.011$; $ES = 0.761$);
– a significant decrease, with a very large effect, of the elbow flexion–extension δ of 10.55 degrees ($p = 0.002$; $ES = 0.971$);

– a significant decrease, with a large effect, of the trunk lateral bending ι of 2.64 degrees ($p = 0.015$; $ES = 0.733$);
– a significant decrease, with a huge effect, of the trunk axial rotation κ of 4.09 degrees ($p < 0.001$; $ES = 1.375$).

The decrease of trunk flexion–extension θ is not significant ($p > 0.05$). The correlation between working heights for the shoulder flexion–extension α and elbow flexion–extension δ is visible in Fig. 10, where the points of *low configuration* tend to be positioned at bottom right, instead, the points of *middle configuration* tend to be positioned at top left. Moreover, the figure notices a small correlation between these angles ($R^2 = 0.515$). The other angles do not have correlations. The correlation between working heights for the trunk angles is indeed visible in Fig. 11, where the points of *low configuration* tend to be positioned at top right; indeed, the points of *middle configuration* tend to be positioned at bottom left, for each considered subject. In summary, we can conclude that the illustrated results show an increase trend of shoulder flexion–extension angle passing from *low configuration* to *middle configuration*; indeed, the other angles decrease.

4.3 Dynamic loads

The effects of loads during the execution of industrial task are taken into consideration through the evaluation of the temporal profiles and the average values of joint torques, as result of the inverse dynamic computation.

Average values of joint torques The average values of the torques of the most activated joints for the two configurations and for the four subjects are illustrated in Fig. 12. The figure does not include the trunk axial rotation torque (τ_{10}) since its variation is very small (less than 0.06 Nm). Moreover, the decrease of trunk flexion–extension θ is not statistically significant. The figure shows that the most loaded joints are trunk lateral bending (τ_9) and shoulder flexion–extension (τ_1). The first result (regarding τ_9) is in accordance with the execution mode of the task since the drilling task is carry out only with dominant hand. The second result (regarding τ_1), instead, is due to an increase in the working height and consequently an increase in the shoulder flexion–extension (α, see Fig 9). Moreover, passing from *low configuration* to *middle configuration*, Fig. 12 underlines:

– a significant increase, with a huge effect, of the shoulder flexion–extension torque τ_1 of 2.18 Nm ($p < 0.001$; $ES = 1.697$);
– a significant decrease, with a large effect, of the shoulder abduction–adduction torque τ_2 of 0.38 Nm ($p = 0.017$; $ES = 0.765$);
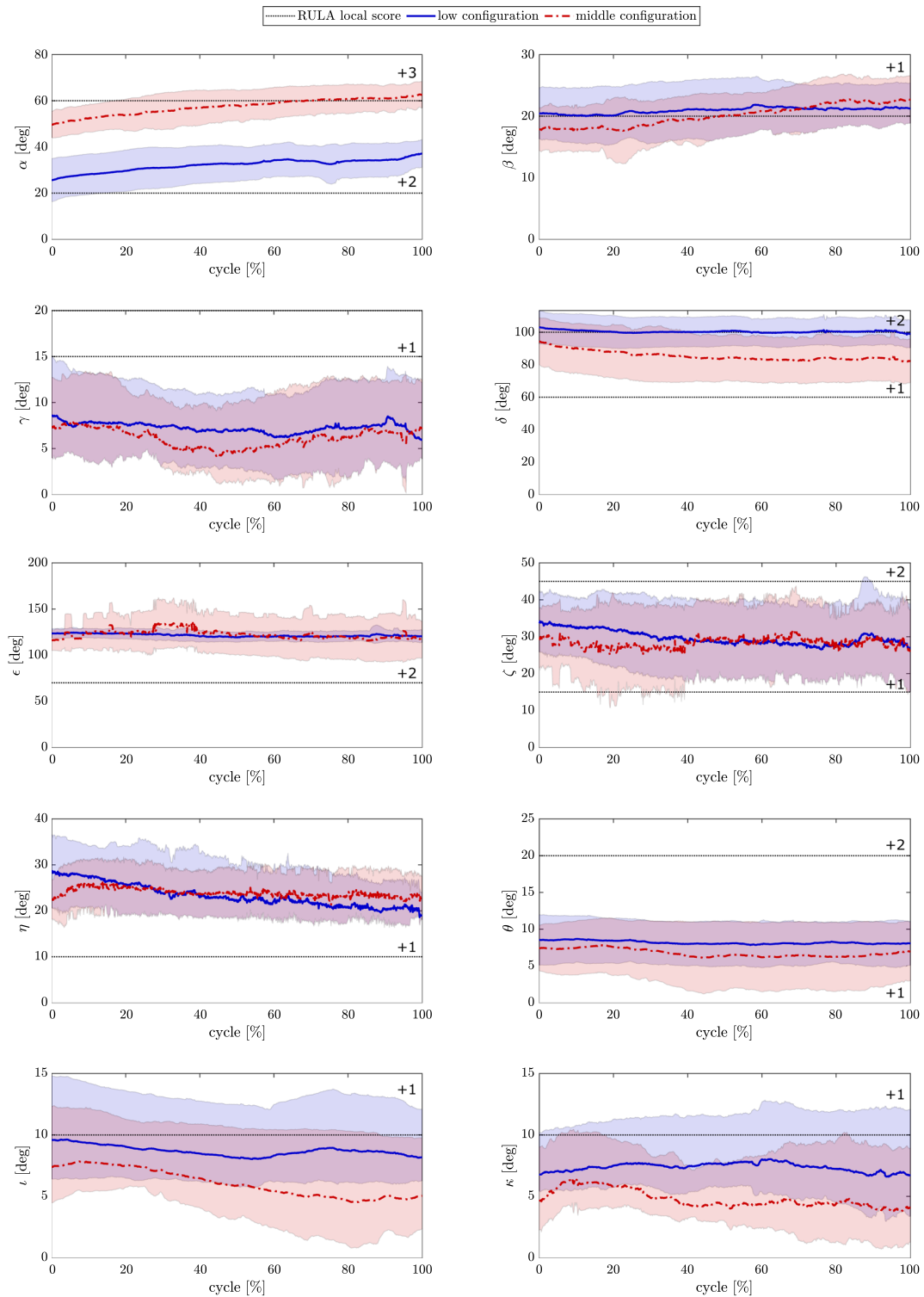
Fig. 9 The evolution over time of joint angles presented as mean ± standard deviation for each configuration (*low configuration* and *middle configuration*)). The joint angles represented in the figure are: α: shoulder flexion-extension; β: shoulder abduction-adduction; γ: shoul-

der rotation; δ: elbow flexion-extension; ϵ: pronation and supination; ζ: wrist flexion-extension; η: wrist radial-ulnar deviation; θ: trunk flexion-extension; ι: trunk lateral bending; κ: trunk axial rotation
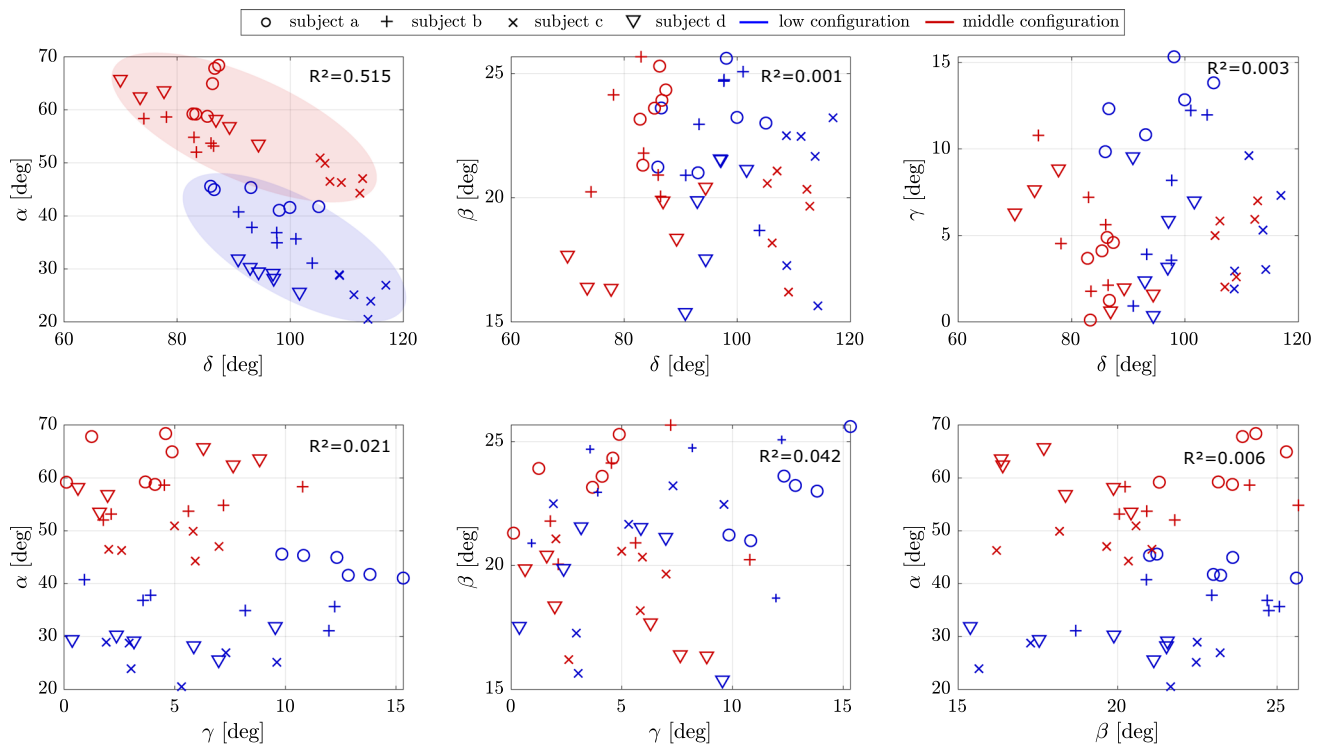
Fig. 10 Average values, for each work cycle, of upper arm joint angles for the two configurations referred to as *low configuration* and *middle configuration*. The mean joint angles represented in the figure are: α: shoulder flexion-extension; β: shoulder abduction-adduction; γ: shoulder rotation; δ: elbow flexion-extension. R^2: linear determination coefficient. For a correct view of these plots, the readers are invited to see the image with colors (colour figure online)
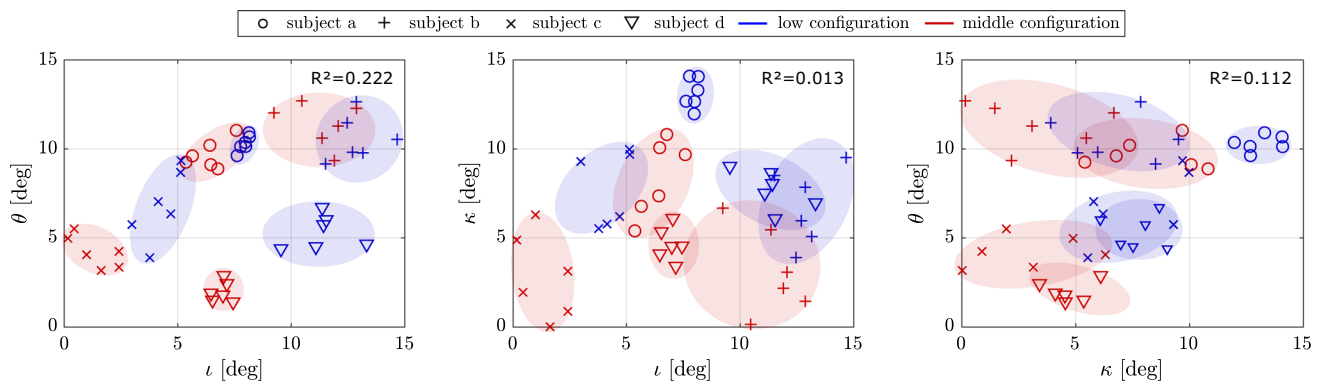

Fig. 11 Average, for each work cycle, of trunk joint angles for the two configurations referred to as *low configuration* and *middle configuration*. The mean joint angles represented in the figure are: θ: trunk flexion-extension; ι: trunk lateral bending; κ: trunk axial rotation. R^2: linear determination coefficient. For a correct view of these plots, the readers are invited to see the image with colors (colour figure online)

- a significant decrease, with a huge effect, of the shoulder rotation torque τ_3 of 0.28 Nm ($p < 0.001$; $ES = 1.311$);
- a significant decrease, with a very large effect, of the elbow flexion-extension torque τ_4 of 0.38 Nm ($p = 0.009$; $ES = 0.842$);
- a significant decrease, with a very large effect, of the trunk lateral bending torques τ_9 of 0.35 Nm ($p = 0.004$; $ES = 0.950$);

4.4 Muscle activities

The biomechanical analysis presented in this paper uses root mean square (RMS) of normalized muscle activation as metric for muscle activities. The results of the muscle activations are used to define the most activated muscle in the two different working height configurations.
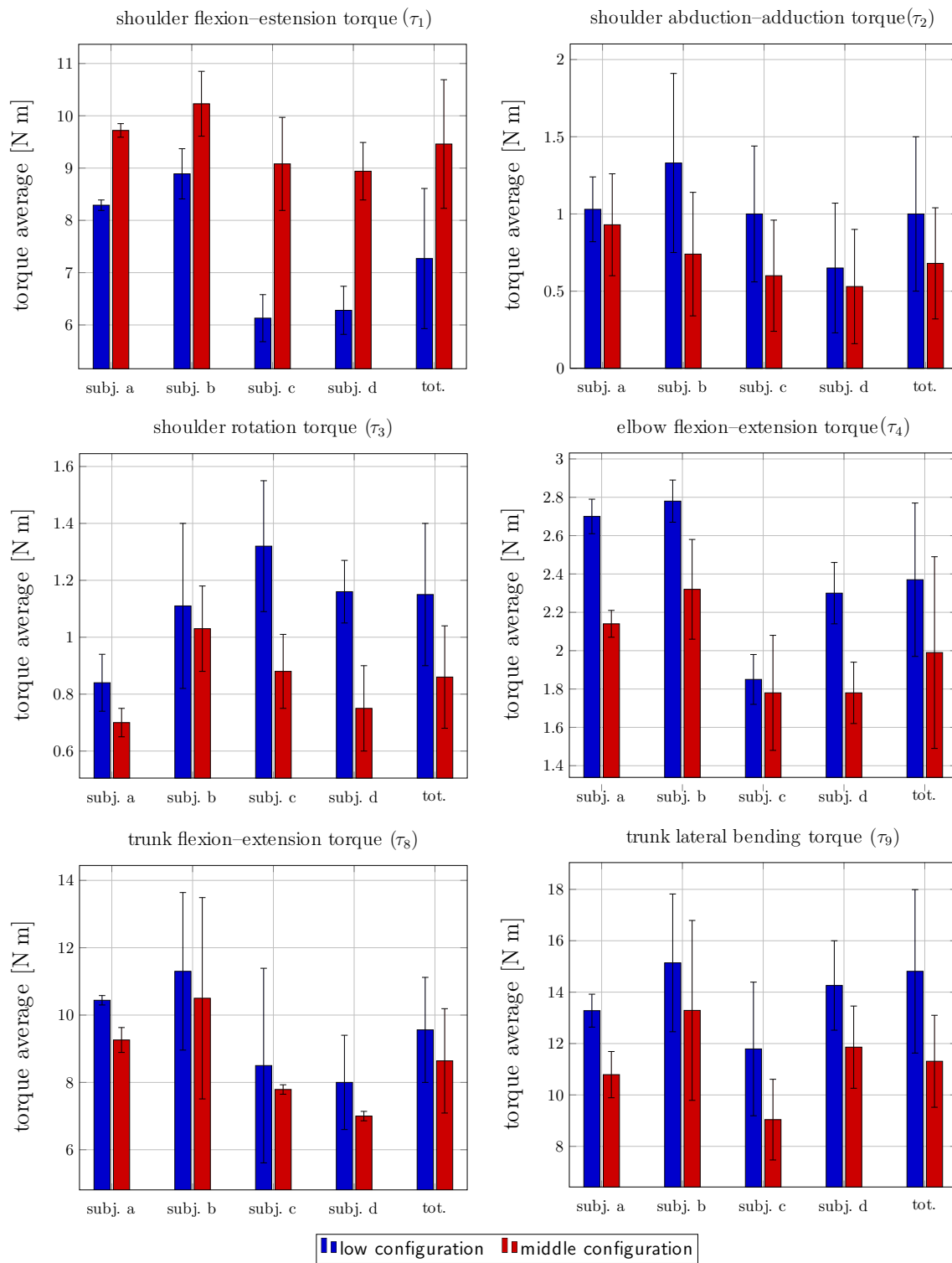
Fig. 12 Average values of the joint torques for the four subjects (subj. a; subj. b; subj. c and subj. d) in two different configurations

RMS of normalized muscle activations The root mean square (RMS) values of the normalized muscle activations (NMA), for all subjects in the two different configurations, are reported in Fig. 13. The decrease and increase of the extensor carpi radials longus (EC) and medial deltoid (MD) are not statistically significant. Moreover, the figure shows that the most activated muscles in *low configurations* are: anterior deltoid (AD) for subject a; biceps brachii (BB) for subject b and d; erector spinae at level L3 ($L3$) for subject c. The most activated muscles in *middle configurations* are: anterior deltoid (AD) for subject a, c and d; upper trapezium (UT) for subject b. As matter of the fact, we can notice:

– a significant increase, with a very large effect, of the anterior deltoid AD muscle activation of 0.14 ($p = 0.005$; $ES = 0.862$);
– a significant increase, with a very large effect, of the upper trapezium UT muscle activation of 0.14 ($p = 0.004$; $ES = 0.873$);
– a significant decrease, with a large effect, of the biceps brachii BB muscle activation of 0.10 ($p = 0.032$; $ES = 0.638$);
– a significant decrease, with a huge effect, of the long head of the triceps brachii TB muscle activation of 0.14 ($p < 0.001$; $ES = 1.635$);
– a significant decrease, with a large effect, of the erector spinae muscle activation at level $L3$ of 0.09 ($p = 0.033$; $ES = 0.631$).
– a significant decrease, with a large effect, of the erector spinae muscle activation at level $T9$ of 0.07 ($p = 0.035$; $ES = 0.627$).

5 Discussion

In this section we present an extensive discussion of the results. We compare the results with respect to standard approaches for ergonomic assessment currently used in industry and comparing works. Then, we present possible exploitation of the results from the industrial perspective. Finally, we conclude the section by presenting the limitations of the work.

5.1 Overall discussion of the results

5.1.1 Task performance

The reduction of movement duration in the *middle configuration* suggests that this configuration of the workstation increases the productivity of drilling overhead tasks (see Fig. 8). High productivity reduces costs for companies and can generate well-being among workers due to an average decrease in the workload of the individual worker.

5.1.2 Kinematic movements

The human joint trajectories are highly affected by the different configurations of the workstation: indeed, as we can see from the pairwise comparison of joint angles (Figs. 10 and 11), passing from *low configuration* to *middle configuration*, the average values of trunk joints (ι and κ), elbow joint (δ), shoulder joints (β and γ) have a significant decrease while the shoulder flexion–extension angle (α) has a significant increases. Moreover, the angles of the shoulder and elbow in the sagittal plane (α and δ) and the trunk angles on the three anatomical planes (θ, ι and κ) have a major correlation on the selected task. In summary, by only using kinematic metrics we are not able to distinguish which configuration is the most comfortable from the ergonomic point of view.

5.1.3 Dynamic loads

The analysis of human joint torques (Fig.12) underlines that the most loaded joints in overhead drilling tasks are: shoulder and trunk joints (τ_1, τ_8 and τ_9). There exists a common trend of the torques relative to the shoulder, elbow and trunk angles. In particular, the increase of shoulder flexion-extension torque (τ_1) and the decrease of elbow flexion–extension (τ_4), trunk flexion–extension and lateral bending (τ_8 and τ_9) are due to an increase and decrease of the relative human joint angles α, δ, θ and ι respectively (see Figs. 9, 10 and 11). Again, using only dynamic metrics, we can individuate the most loaded joint but, it is difficult to discriminate the optimal configuration of the workstation. Moreover, the same results are obtained by using the most adopted ergonomic method in industry (i.e. RULA method) and they are also shown in the previous works presented in the literature (see Sect. 5.2).

5.1.4 Muscle activities

There exists a common trend of the muscle activations relative to the shoulder, elbow and trunk torques. In particular, the increase of anterior deltoid (AD) and medial deltoid (MD) and the decrease of biceps brachii (BB), long head of the triceps brachii (TB), erector spinae at level L3 and T9 ($L3$ and $T9$) are due to increase and decrease of the relative human joint torques τ_1, τ_4, τ_8 and τ_9 (see Fig.12). The normalized muscle activations of upper trapezius (UT) have a significant increase passing from the *low configuration* to the *middle configuration*. This trend cannot be caused by an increase neck torques since, for the selected task, they are very small. For this reason, this trend could be caused by an isometric contraction of the muscle during the execution of the activity. The same results are also shown in the previous studies present in the literature (see Sect. 5.2). We can conclude that the RMS values of normalized muscle acti-

Fig. 13 Root mean square (RMS) of the normalized muscle activation (NMA) values for the four subjects (subj. a; subj. b; subj. c and subj. d) in two different configurations
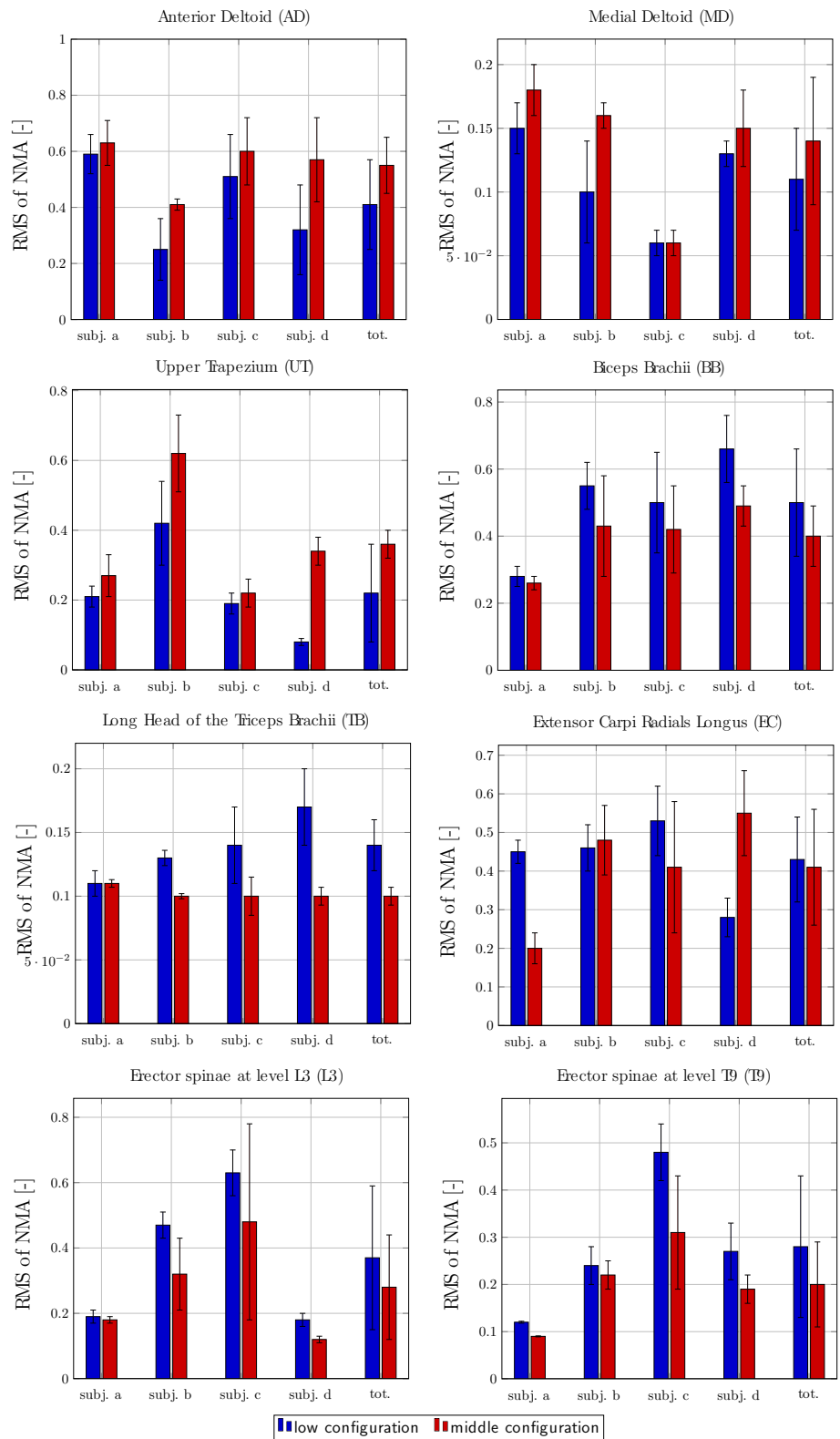
vations (Fig. 13 and Table 2) indicate that: shoulder/neck body muscles, arm/hand body muscles and trunk/lower back body muscles are the most activated in the *low configuration*; indeed, in the *middle configuration*, the most activated muscles refer only to shoulder/neck body muscles. Thus, from the muscle activities point of view, the *middle configuration* seems the best working configuration for workers. The latter configuration causes the isolation of the most activated muscles in a single muscle areas, and therefore it is possible to selectively act in this are to reduce worker muscle activities (see Sect. 5.3).

5.2 Comparison with RULA method and compering works

The biomechanical analysis considered in this work has been compared with the RULA ergonomic assessment method and with compering works.

RULA method We have selected RULA method since we are interested in industrial tasks that only concern the upper body, and the RULA method is the standard approach used in current industries for evaluating the risks associated to WMSD. Table 3 shows the results of the RULA local scores and RULA final scores for each work cycle and for the two working heights. The distribution of the RULA final scores for the different configurations are: in 79.2% of the *low configuration* cases the RULA final score is equal to 7 and in 75% of the *middle configuration* cases the score is always equal to 7. In agreement with [9,14], the task performance increase in the highest working configuration. A correlation between execution time and ergonomic risks is reported in [14]. The study indicates that an increase in task performance carries a lower ergonomic risk in terms of RULA score. In our study, in contrast to the study presented in [14], we do not observe significant difference in terms of RULA score for the two different working heights. The discrepancy between the studies is due to the percentage of height variation; in our case the variation in the average working height is equal to 9% and it is smaller then the variation presented in [14] which is equal to 33%. Figure 9 plots the limits of RULA over the joint trajectories reconstructed using inverse kinematics for this specific task and working configurations. In particular, from our kinematic metrics we have noticed an increased value of shoulder flexion–extension angle passing from *low configuration* to *middle configuration*, and decreased values of trunk angles (see Sect. 4.2): these angle variations are not causing a changing of the RULA local, and thus, final scores (see Table 3), since the ranges of RULA method are not sensitive to small variations, which can also indicate useful results about human ergonomics. Indeed, this is confirmed by the inverse dynamic results: even a small variation of these angles causes a significant variation of the joint torques, especially for trunk angles.

In summary, the RULA local and final scores alone, for this task and working configurations, do not allow to understand which configuration could potentially minimize the WMSD risks for the worker and to define the difference between the two configurations.

Compering works The previous studies presented in the literature to estimate the loads and muscle activities of the worker during the execution of overhead drilling task in the same working height configuration highlight the equal difficulties encountered in this work [8,9]. In particular, the first study [8] shows the effect of the working heights on shoulder toque and muscle activations. The authors propose to perform a static two-dimensional analysis to estimate the joint torque of the shoulder and the EMG analysis of three different muscles (anterior deltoid AD, biceps brachii BB and long head of the triceps brachii TB) during the execution of the task. The RMS of EMG signal and average values of torque are used as performance metrics. Passing from lower configuration to higher configuration, the results show a significant increase of shoulder torque of 6.04 Nm, a significant increase of muscle activations of anterior deltoid (AD) of 10.8% and a significant decrease of biceps brachii (BB) of 21.7%. The trend of results are in agreement with the results presented in this work, increasing the working height the shoulder muscles overload; the difference between the values of joint torque and muscle activations, could be due to the different weight of the drill used for the experiments. The second study [9], instead, illustrates the effect of working heights on shoulder muscle activities. The authors propose to perform EMG analysis of the muscles in the shoulder region. In particular, the EMG signal of anterior deltoid (AD), medial deltoid (MD) and upper trapezium (UT) muscles were acquired during a simulated overhead drilling task in different heights and the performance metric selected is maximum voluntary contraction. The results presented in this study [9] do not allow to notify a significant effects of working height on EMG-based muscle activities. The discrepancy between these results and the results presented in the present work may be due to the different selected metrics. The metric selected for the present study is RMS of NMA and it calculates the area under the curve taking into consideration the evolution over time of the NMA. The metric selected in [9], instead, is the maximum of NMA and it takes into account only the maximum value of the muscle activation. It is important to underline that both previous studies focus on the static shoulder torque and upper arm muscle activities, not considering the effect of height on the trunk muscle activities which, as shown in this study, decrease passing from *low configuration* to *middle configuration*.

In summary: (i) our study considers a complete biomechanical analysis involving the analysis of joint kinematics and dynamics as well as muscle activities; (ii) our study includes joint angles, torques and muscles of the whole upper

Table 3 The table shows the RULA local and final score for drilling overhead task

Drilling task																						
RULA local score [–]																				RULA final score [–]		
Upper arm				Lower arm				Wrist				Trunk				Neck						
a	b	c	d	a	b	c	d	a	b	c	d	a	b	c	d	a	b	c	d	a	b	c	d
Low configuration																							
WC 1.1	3	3	3	3	3	2	2	2	4	4	5	5	2	2	1	2	1	1	1	1	**7**	**7**	**6**	**7**
WC 1.2	3	3	3	3	3	2	2	2	4	4	5	5	2	3	2	2	1	1	1	1	**7**	**7**	**7**	**7**
WC 1.3	3	3	3	3	3	2	2	2	4	4	5	5	2	3	2	2	1	1	1	1	**7**	**7**	**7**	**7**
WC 2.1	3	3	3	3	3	3	2	2	4	4	5	5	2	3	1	2	1	1	1	1	**7**	**7**	**6**	**7**
WC 2.2	3	3	3	3	3	3	2	2	4	4	5	5	2	3	1	2	1	1	1	1	**7**	**7**	**6**	**7**
WC 2.3	3	3	3	2	3	3	2	2	4	5	5	5	2	2	1	2	1	1	1	1	**7**	**7**	**6**	**6**
Middle configuration																							
WC 1.1	4	4	3	4	1	2	2	1	4	5	5	4	2	2	2	2	1	1	1	1	**7**	**7**	**7**	**7**
WC 1.2	4	4	3	4	1	2	2	1	4	5	5	4	2	2	1	2	1	1	1	1	**7**	**7**	**6**	**7**
WC 1.3	4	4	3	4	1	2	2	1	4	5	5	3	2	2	1	2	1	1	1	1	**7**	**7**	**6**	**7**
WC 2.1	4	4	3	4	1	3	2	1	4	4	5	4	1	2	1	2	1	1	1	1	**6**	**7**	**6**	**7**
WC 2.2	4	4	3	3	1	3	2	1	4	4	5	4	1	2	2	2	1	1	1	1	**6**	**7**	**7**	**7**
WC 2.3	4	4	3	3	1	3	2	1	4	4	5	3	1	2	2	2	1	1	1	1	**6**	**7**	**7**	**7**

The letters a, b, c and d represent the four subjects and WC represents work cycle of the trial

body; (ii) our results suggest that different working heights have an impact not only on the joints and muscles of the upper-limb, but also on the joints and muscles of the trunk.

5.3 Possible exploitation of the results

The results of these works can be exploited at different levels, with increasing complexity. Indeed, the proposed analysis can be used for multiple applications: (i) biomechanical analysis of existing industrial workstations; (ii) developing synthetic biomechanical indices [47] for user-centered ergonomic evaluation of industrial tasks [48]; (iii) providing guidelines for the design of novel human-oriented industrial workstations [11]; (iv) providing guidelines for design of novel human- and task-oriented assistive devices [49,50].

In particular, the results of this study suggest that the *middle configuration* reduces the joint angles/torques of the trunk and elbow (see Sect. 4.3 and Sect. 4.4). However, this configuration implicates an increase of shoulder flexion-extension angle and torque. This seems a problem, but the important aspect is that in the *middle configuration* the most activated muscles are concentrated in a specific part of the body (shoulder/neck body muscles), differently from the *low configuration* where it is not possible to find this discrepancy and thus isolate the source of WMSD. This results is important since it allows to state that, for overhead tasks, the best configuration is the *middle configuration*, with the possibility to provide selective assistance in this anatomical area with wearable robots reducing the risks associated to the WMSD [10,51].

5.4 Limitation of the study

This preliminary work present some limitations. The first limitation is related to the sample size that was performed for the experiments. A limited number of subjects were involved since only an analysis of this type allowed to identify the most activated muscle of each subject, for each work configuration selected. The second limitation is the nature of the subjects involved for the experiments. The subjects were selected based on their anthropometric characteristics, but they do not have or have limited experience with overhead industrial tasks. However, many other preliminary studies do not use real workers [2,9,14,20] and therefore the results from inexperienced subjects can be considered as valid as those of the previous works.

6 Conclusions

The evaluation of demanding tasks as overhead drilling requires a complete biomechanical analysis of the workers, in order to define the most loaded joints and muscles, with the final goal of providing ergonomic guidelines for the workers. The analysis reported in this study allows to understand in details which are the areas of the body subjected to major stress, and thus can provide information on the real source of WMSD. The results shows that the highest working configuration, defined as *middle configuration*, may help in reducing strain on trunk and upper arm, but causes an increased shoulder strain. Another important aspect is that overhead works are very complex tasks to be studied, and it is difficult to

find a workplace solution that minimizes the risk associated to WMSD. Future works are needed in order to verify the possible exploitation of the results presented in this study, in terms of user-centered design of the workstation or user-centered design of assistive devices, i.e. robotic exoskeletons. With this regard, the use of robotic exoskeletons is preferable in the *middle configuration* since at this working height the most activated muscles are in a single muscle area, and thus, it is simpler to provide assistance at this area with a wearable robotic device.

A Modeling

In this appendix the procedures for inverse kinematic and inverse dynamic computation starting from the motion capture and ground reaction forces data, are reviewed.

A.1 Inverse kinematics

The inverse kinematics aims at computing the evolution over time of the joint angles. Here, the problem is to minimize the weighted squared error between the motion capture data and the virtual model [12], as

$$\min_q = \sum_{i=1}^{o} \omega_i (x_{i,s} - x_{i,m})^2 + \sum_{j=1}^{n} \omega_j (q_{j,s} - q_{j,m})^2 \quad (2)$$

where ω_i and ω_j: weight coefficients for markers and joint angles, respectively; $x_{i,s}$ and $x_{i,m}$: three dimensional positional vectors of the ith marker, respectively for the subject and the model ($x \in \mathbb{R}^n$); $q_{j,s}$ and $q_{j,m}$: three dimensional vectors of generalized coordinates (unknowns) of the jth joint angle, respectively for the subject and the model ($q \in \mathbb{R}^n$). n, o: respectively, degrees-of-freedom (DoF) of the model (i.e. number of considered joint angles) and number of markers.
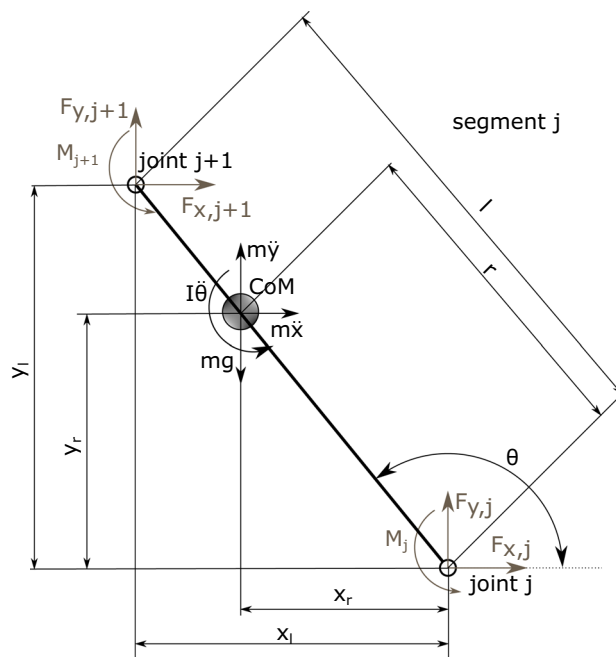

Fig. 14 Schematic model of the generic body segment between two human joints

A.2 Inverse dynamics

The inverse dynamics aims at computing the evolution over time of the joint torques, starting from the joint angles computed according to the procedure defined in A.2 and the measured ground reaction forces. By neglecting the viscous and friction effects, the dynamic model takes the classic Lagrangian form:

$$M(q)\ddot{q} + c(q, \dot{q}) + g(q) = \tau \quad (3)$$

where $q, \dot{q}, \ddot{q}$: position, velocity, and acceleration of the generalized coordinates ($q \in \mathbb{R}^n$); M: mass matrix ($M \in \mathbb{R}^{n \times n}$); c: vector of Coriolis and centrifugal forces ($c \in \mathbb{R}^n$); g: vector of gravitational forces ($g \in \mathbb{R}^n$); τ: vector of unknown generalized forces ($\tau \in \mathbb{R}^n$).

The dynamic model (3) can be also written in Newton–Euler formulation as:

$$x, \dot{x}, \ddot{x} \rightarrow \sum F_x = m\ddot{x}$$

$$y, \dot{y}, \ddot{y} \rightarrow \sum F_y = m\ddot{y} \quad (4)$$

$$\theta, \dot{\theta}, \ddot{\theta} \rightarrow \sum M = I\ddot{\theta}$$

where F_x: forces along x; m: mass of the human segment; $\ddot{x}$: linear acceleration along x; F_y: forces along y; $\ddot{y}$: linear
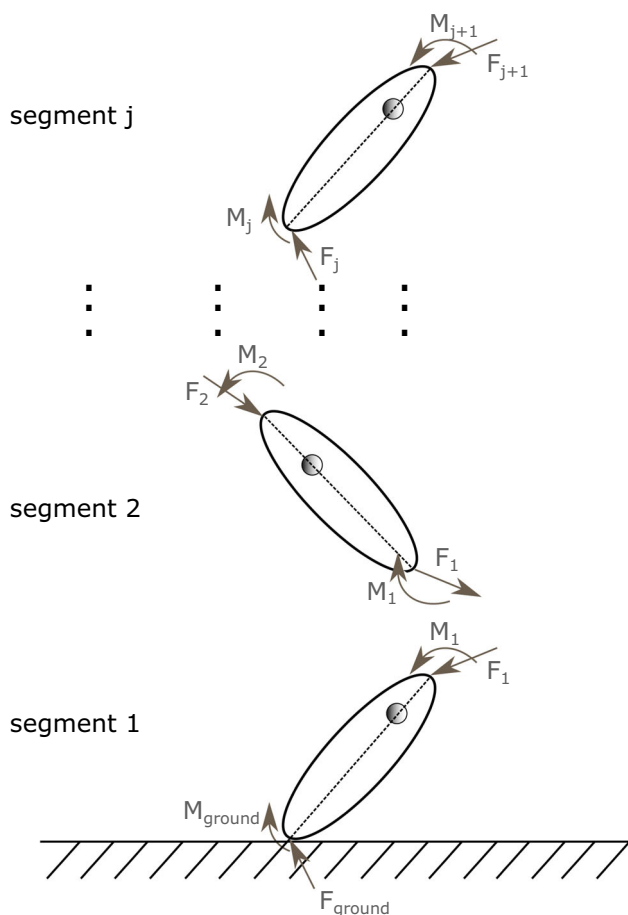
Fig. 15 Graphical model of the inverse dynamics calculation of joint forces and torques for each segment

acceleration along y; M: moment; I: mass moment of inertia; $\ddot{\theta}$: angular acceleration.

By considering a generic body segment (segment j) which links two consecutive human joints (joint j and joint $j + 1$) and, by considering the nomenclature in Fig. 14, we can re-write the dynamic model (4) in two different ways:

$$
\begin{aligned}
F_{x,j+1} &= m\ddot{x} - F_{x,j} \\
F_{y,j+1} &= m\ddot{y} - mg - F_{y,j} \\
M_{j+1} &= I\ddot{\theta}_j - M_j - F_{x,j+1}(y_l - y_r) + F_{y,j+1}(x_l - x_r) \\
&\quad + F_{y,j} y_r - F_{x,j} x_r
\end{aligned} \tag{5}
$$

$$
\begin{aligned}
F_{x,j+1} &= m\ddot{x} - F_{x,j} \\
F_{y,j+1} &= m\ddot{y} - mg - F_{y,j} \\
M_{j+1} &= I\ddot{\theta}_j - M_j - F_{x,j+1}(l - r)S(\theta) \\
&\quad + F_{y,j+1}(l - r)C(\theta) \\
&\quad + F_{y,j} r C(\theta) - F_{x,j} r S(\theta)
\end{aligned} \tag{6}
$$

In (5) and (6), the forces due to the acceleration of the mass along x and y axes (i.e., $m\ddot{x}$ and $m\ddot{y}$), as well as the weight

force mg are applied in the center of mass (CoM) of the considered body segment. The moment of inertia $I\ddot{\theta}$ is also considered about the CoM. Instead, the internal generalised forces (i.e., forces F_j and F_{j+1}; torques M_j and M_{j+1}), are applied at the joints location (joint j and $j + 1$).

Equation 5 depends on the distances between the CoM and the joints along x and y axes (y_r and y_l; x_r and x_l); instead, Eq. 6 depends on the joint angle θ. Starting from the segment 1, where the ground reaction forces are known, it is possible to reconstruct the forces and torques applied at each human joint (see Fig. 15 for a graphical interpretation).

References

1. Schneider, E., Irastorza, X.: Osh in Figures: Work-Related Musculoskeletal Disorders in the EU—Facts and Figures. European Agency for Safety and Health at Work
2. Maurice, P. et al., Objective and Subjective Effects of a Passive Exoskeleton on Overhead Work. In: Proceedings of the IEEE Transactions on Neural Systems and Rehabilitation Engineering, vol. 28, no. 1, pp. 152–164 (2020). https://doi.org/10.1109/TNSRE.2019.2945368
3. Karhu, O., Kansi, P., Kuorinka, I.: Correcting working postures in industry: a practical method for analysis. Appl. Ergon. **8**(4), 199–201 (1977)
4. McAtamney, L., Corlett, E.N.: RULA: a survey method for the investigation of work-related upper limb disorders. Appl. Ergon. **24**(2), 91–99 (1993)
5. Hignett, S., McAtamney, L.: Rapid Entire Body Assessment (REBA). Appl. Ergonomics, **31**, 201–205 (2000). https://doi.org/10.1016/S0003-6870(99)00039-3
6. Panariello, D., Grazioso, S., Caporaso, T., Palomba, A., Di Gironimo, G., Lanzotti, A.: Evaluation of human joint angles in industrial tasks using opensim. In: II Workshop on Metrology for Industry 4.0 and IoT (MetroInd4. 0&IoT), pp. 78–83. IEEE (2019)
7. Maurice, P., Malaisé, A., Amiot, C., Paris, N., Richard, G.-J., Rochel, O., Ivaldi, S.: Human movement and ergonomics: an industry-oriented dataset for collaborative robotics. Int. J. Robot. Res. **38**(14), 1529–1537 (2019)
8. Anton, D., Shibley, L.D., Fethke, N.B., Hess, J., Cook, T.M., Rosecrance, J.: The effect of overhead drilling position on shoulder moment and electromyography. Ergonomics **44**(5), 489–501 (2001)
9. Sood, D., Nussbaum, M.A., Hager, K.: Fatigue during prolonged intermittent overhead work: reliability of measures and effects of working height. Ergonomics **50**(4), 497–513 (2007)
10. Caporaso, T., Grazioso, S., Panariello, D., Di Gironimo, G., Lanzotti, A.: Understanding the human motor control for user-centered design of custom wearable systems: case studies in sports, industry, rehabilitation. In: International Conference on Design, Simulation, Manufacturing: The Innovation Exchange, pp. 753–764. Springer (2019)
11. Panariello, D., Grazioso, S., Caporaso, T., Di Gironimo, G., Lanzotti, A.: User-centered approach for design and development of industrial workplace. Int. J. Interact. Des. Manuf. **15**(1), 121–123 (2021). https://doi.org/10.1007/s12008-020-00737-x
12. Delp, S.L., Anderson, F.C., Arnold, A.S., Loan, P., Habib, A., John, C.T., Guendelman, E., Thelen, D.G.: Opensim: open-source software to create and analyze dynamic simulations of movement. IEEE Trans. Biomed. Eng. **54**(11), 1940–1950 (2007)

13. Spada, S., Ghibaudo, S., Gilotta, S., Gastaldi, L., Cavatorta, M.P.: Analysis of exoskeleton introduction in industrial reality: main issues and EAWS risk assessment. In: International Conference on Applied Human Factors and Ergonomics, pp. 236–244. Springer (2017)

14. Alabdulkarim, S., Nussbaum, M.A., Rashedi, E., Kim, S., Agnew, M., Gardner, R.: Impact of task design on task performance and injury risk: case study of a simulated drilling task. Ergonomics **60**(6), 851–866 (2017)

15. Peruzzini, M., Pellicciari, M., Gadaleta, M.: A comparative study on computer-integrated set-ups to design human-centered manufacturing systems. Robot. Comput. Integr. Manuf. **55**, 265–278 (2019)

16. Sylla, N., Bonnet, V., Colledani, F., Fraisse, P.: Ergonomic contribution of able exoskeleton in automotive industry. Int. J. Ind. Ergon. **44**(4), 475–481 (2014)

17. Georgarakis, A.-M., Wolf, P., Riener, R.: Simplifying exosuits: kinematic couplings in the upper extremity during daily living tasks. In: 2019 IEEE 16th International Conference on Rehabilitation Robotics (ICORR), pp. 423–428. IEEE (2019)

18. Kim, W., Lee, J., Peternel, L., Tsagarakis, N., Ajoudani, A.: Anticipatory robot assistance for the prevention of human static joint overloading in human–robot collaboration. IEEE Robot. Autom. Lett. **3**(1), 68–75 (2017)

19. Kim, W., Lorenzini, M., Kapıcıoğlu, K., Ajoudani, A.: Ergotac: a tactile feedback interface for improving human ergonomics in workplaces. IEEE Robot. Autom. Lett. **3**(4), 4179–4186 (2018)

20. Blache, Y., Desmoulins, L., Allard, P., Plamondon, A., Begon, M.: Effects of height and load weight on shoulder muscle work during overhead lifting task. Ergonomics **58**(5), 748–761 (2015)

21. Maciukiewicz, J.M., Cudlip, A.C., Chopp-Hurley, J.N., Dickerson, C.R.: Effects of overhead work configuration on muscle activity during a simulated drilling task. Appl. Ergon. **53**, 10–16 (2016)

22. Bruno, F., Barbieri, L., Muzzupappa, M.: A mixed reality system for the ergonomic assessment of industrial workstations. Int. J. Interact. Des. Manuf. (IJIDeM) **14**(3), 805–812 (2020)

23. Di Gironimo, G., Caporaso, T., Del Giudice, D.M., Tarallo, A., Lanzotti, A.: Development of a new experimental protocol for analysing the race-walking technique based on kinematic and dynamic parameters. Proc. Eng. **147**, 741–746 (2016)

24. Conforti, I., Mileti, I., Panariello, D., Caporaso, T., Grazioso, S., Del Prete, Z., Lanzotti, A., Di Gironimo, G., Palermo, E.: Validation of a novel wearable solution for measuring l5, s1 load during manual material handling tasks. In: IEEE International Workshop on Metrology for Industry 4.0 & IoT, pp. 501–506. IEEE (2020)

25. Kim, D., Kwon, J., Han, S., Park, Y.-L., Jo, S.: Deep full-body motion network for a soft wearable motion sensing suit. IEEE/ASME Trans. Mechatron. **24**(1), 56–66 (2018)

26. Muro-De-La-Herran, A., Garcia-Zapirain, B., Mendez-Zorrilla, A.: Gait analysis methods: an overview of wearable and non-wearable systems, highlighting clinical applications. Sensors **14**(2), 3362–3394 (2014)

27. Roetenberg, D., Luinge, H., Slycke, P.: Xsens mvn: full 6dof human motion tracking using miniature inertial sensors. Xsens Motion Technologies BV, Technical report 1

28. Schepers, H.M., Koopman, H.F., Veltink, P.H.: Ambulatory assessment of ankle and foot dynamics. IEEE Trans. Biomed. Eng. **54**(5), 895–902 (2007)

29. Palermo, E., Rossi, S., Marini, F., Patanè, F., Cappa, P.: Experimental evaluation of accuracy and repeatability of a novel body-to-sensor calibration procedure for inertial sensor-based gait analysis. Measurement **52**, 145–155 (2014)

30. Raschke, U.: The Jack Human Simulation Tool, Working Postures and Movements-Tools for Evaluation and Engineering, pp. 431–437. CRC Press LLC, Boca Raton (2004)

31. Caporaso, T., Grazioso, S., Panariello, D., Ruggiero, R., Palomba, A., Di Gironimo, G.: Enhancing joint torque estimation of the workers using 3d body models. In: IEEE International Workshop on Metrology for Industry 4.0 & IoT (MetroInd4. 0&IoT), pp. 444–448. IEEE (2021)

32. Damsgaard, M., Rasmussen, J., Christensen, S.T., Surma, E., De Zee, M.: Analysis of musculoskeletal systems in the anybody modeling system. Simul. Model. Pract. Theory **14**(8), 1100–1111 (2006)

33. Maurice, P.: Virtual Ergonomics for the Design of Collaborative Robots. Ph.D. thesis (2015)

34. Chang, J.: The Risk Assessment of Work-Related Musculoskeletal Disorders Based on Opensim. Ph.D. thesis (2018)

35. Cacciari, E., Milani, S., Balsamo, A., Spada, E., Bona, G., Cavallo, L., Cerutti, F., Gargantini, L., Greggio, N., Tonini, G., et al.: Italian cross-sectional growth charts for height, weight and BMI (2 to 20 yr). J. Endocrinol. Investig. **29**(7), 581–593 (2006)

36. Spada, S., Castellone, R., Cavatorta, M.P.: "La fabbrica si misura": an anthropometric study of workers at FCA Italian plants. In: Congress of the International Ergonomics Association, pp. 389–397. Springer (2018)

37. Dahmen, C., Hefferle, M.: Application of Ergonomic Assessment Methods on an Exoskeleton Centered Workplace. In: Proceedings of the XXXth Annual Occupational Ergonomics and Safety Conference, Pittsburgh, PA, USA, 7–8 June 2018

38. Manghisi, V.M., Uva, A.E., Fiorentino, M., Bevilacqua, V., Trotta, G.F., Monno, G.: Real time RULA assessment using kinect v2 sensor. Appl. Ergon. **65**, 481–491 (2017)

39. van Sint Jan, S.: Color Atlas of Skeletal Landmark Definitions E-Book: Guidelines for Reproducible Manual and Virtual Palpations. Elsevier Health Sciences, Amsterdam (2007)

40. Silder, A., Whittington, B., Heiderscheit, B., Thelen, D.G.: Identification of passive elastic joint moment-angle relationships in the lower extremity. J. Biomech. **40**(12), 2628–2635 (2007)

41. Huysamen, K., Bosch, T., de Looze, M., Stadler, K.S., Graf, E., O'Sullivan, L.W.: Evaluation of a passive exoskeleton for static upper limb activities. Appl. Ergon. **70**, 148–155 (2018)

42. Rajagopal, A., Dembia, C.L., DeMers, M.S., Delp, D.D., Hicks, J.L., Delp, S.L.: Full-body musculoskeletal model for muscle-driven simulation of human gait. IEEE Trans. Biomed. Eng. **63**(10), 2068–2079 (2016)

43. Mortensen, J. D., Vasavada, A. N., & Merryweather, A. S.: The inclusion of hyoid muscles improve moment generating capacity and dynamic simulations in musculoskeletal models of the head and neck. PLoS ONE **13**(6) (2018). https://doi.org/10.1371/journal.pone.0199912

44. Grazioso, S., Caporaso, T., Palomba, A., Nardella, S., Ostuni, B., Panariello, D., Di Gironimo, G., Lanzotti, A.: Assessment of upper limb muscle synergies for industrial overhead tasks: a preliminary study. In: II Workshop on Metrology for Industry 4.0 and IoT (MetroInd4. 0&IoT), pp. 89–92. IEEE (2019)

45. Cohen, J.: Statistical Power Analysis for the Behavioral Sciences. Lawrence Erlbaum, ISBN 10: 0121790606 ISBN 13: 9780121790608 (1977)

46. Sawilowsky, S.S.: New effect size rules of thumb. J. Mod. Appl. Stat. Methods **8**(2), 26 (2009)

47. Caporaso, T., Grazioso, S., Di Gironimo, G., Lanzotti, A.: Biomechanical indices represented on radar chart for assessment of performance and infringements in elite race-walkers. Sports Eng. **23**(1), 1–8 (2020)

48. Lanzotti, A., Vanacore, A., Tarallo, A., Nathan-Roberts, D., Coccorese, D., Minopoli, V., Carbone, F., d'Angelo, R., Grasso, C., Di Gironimo, G., et al.: Interactive tools for safety 4.0: virtual ergonomics and serious games in real working contexts. Ergonomics **63**(3), 324–333 (2020)

49. Panariello, D., Grazioso, S., Caporaso, T., Di Gironimo, G., Lanzotti, A.: Preliminary requirements of a soft upper-limb exoskeleton for industrial overhead tasks based on biomechanical analysis. In: Congress of the International Ergonomics Association, pp. 317–324. Springer (2021)

50. Panariello, D., Grazioso, S., Caporaso, T., Gironimo, G.D., Lanzotti, A.: A detailed analysis of the most promising concepts of soft wearable robots for upper-limb. In: International Conference on Design, Simulation, Manufacturing: The Innovation Exchange, pp. 71–81. Springer (2021)

51. Wirekoh, J., Valle, L., Pol, N., Park, Y.-L.: Sensorized, flat, pneumatic artificial muscle embedded with biomimetic microfluidic sensors for proprioceptive feedback. Soft Robot. **6**(6), 768–777 (2019)